University of Baghdad
College of Engineering
JOURNAL OF ENGINEERING

Journal of Engineering

journal homepage: www.joe.uobaghdad.edu.iq

Volume 29 Number 10 October 2023

Numerical Assessment of Pipe Pile Axial Response under Seismic Excitation

Duaa Al-Jeznawi[1] , Ismacahyadi B. Mohamed Jais[2,*], Bushra S. Albusoda[3], Norazlan Khalid[4]

[1] Department of Civil Engineering, College of Engineering, Al-Nahrain University, Jadriya, Baghdad, Iraq.
[1,2,4]School of Civil Engineering, College of Engineering, Universiti Teknologi MARA Shah Alam, 40450, Selangor, Malaysia
[3] Department of Civil Engineering, College of Engineering, University of Baghdad, Baghdad, Iraq.
duaa.a.al-jeznawi@nahrainuniv.edu.iq[1], ismac821@uitm.edu.my[2],
dr.bushra_albusoda@coeng.uobaghdad.edu.iq[3], norazlan0481@salam.uitm.edu.my[4]

ABSTRACT

In engineering, the ground in seismically active places may be subjected to static and seismic stresses. To avoid bearing capacity collapse, increasing the system's dynamic rigidity, and/or reducing dynamic fluctuations, it may be required to employ deep foundations instead of shallow ones. The axial aptitude and pipe pile distribution of load under static conditions have been well reported, but more study is needed to understand the dynamic axial response. Therefore, this research discusses the outputs of the 3D finite element models on the soil-pile behavior under different acceleration intensities and soil states by using MIDAS GTS NX. The pipe pile was represented as a simple elastic, and a modified Mohr-Coulomb model was used to describe the surrounding soil layers. When low acceleration was introduced in the early stages, positive frictional resistance (i.e., in dry soil, the FR was about 1.61, 1.98, and 0.9 Mpa under Kobe, Halabja, and Ali Algharbi earthquakes, respectively) was recorded. However, as the acceleration increased (from PGA of 0.1 g and 0.102 g to 0.82 g), the resistance reduced and eventually turned negative. In this study, both internal and exterior frictional resistance were measured. It was found that the soil state and acceleration intensity both have a noticeable effect on the failure process, i.e., the maximum plug soil resistance decreased by about 55% by changing the soil condition from a dry to a saturated state under the recorded data of the Kobe earthquake. A rough estimation of the long-term settlements at the shaken soil surface is meant to be included in the results of this research.

Keywords: Axial response, Seismic load, 3D finite element, Frictional resistance, Settlement.

*Corresponding author
Peer review under the responsibility of University of Baghdad.
https://doi.org/10.31026/j.eng.2023.10.01

Article received: 25/03/2023
Article accepted: 04/08/2023
Article published: 01/10/2023

التقييم العددي للاستجابة المحورية للركيزة الأنبوبية تحت الإثارة الزلزالية

دعاء الجيزناوي[1]، اسماكيادي[2،*]، بشرى سهيل البوسودة[3]، نورزلان خالد[4]

[1]قسم الهندسة المدنية، كلية الهندسة، جامعة النهرين, بغداد، العراق

[1،2،4] هندسة مدنية، كلية الهندسة، جامعة تكنلوجيا مارا شاه علام ، سيلانكور، ماليزيا

[3]قسم الهندسة المدنية، كلية الهندسة، جامعة بغداد, بغداد، العراق

الخلاصة

هندسيا، قد تتعرض التربة في الأماكن النشطة زلزاليًا لكل من الضغوط الساكنة والزلزالية. لغرض تجنب انهيار قدرة التحمل، وزيادة الصلابة الديناميكية لكل من التربة والمنشأ المقام عليها، وتقليل التقلبات الديناميكية، قد يكون من الضروري في هذه الحالة استخدام أساسات عميقة بدلاً من الأسس الضحلة. تم التحري عن الكفاءة المحورية وتوزيع الحمل تحت الظروف الثابتة بشكل جيد، ولكن هناك حاجة إلى مزيد من الدراسة لفهم الاستجابة المحورية الديناميكية للاسس العميقة (الركائز). لذلك، يناقش هذا البحث مخرجات نماذج العناصر المحدودة ثلاثية الأبعاد على سلوك الركائز–التربة تحت شدة تسارع مختلفة في تربة مشبعة. تم تمثيل الركيزة على أنها مادة مرنة بسيطة، وتم استخدام نموذج Mohr-Coulomb المعدل لتمثيل طبقات التربة المحيطة. في المراحل المبكرة، تم تسجيل مقاومة احتكاك موجبة عند التسارع المنخفض. ومع زيادة التسارع، تقل المقاومة وتحولت في النهاية إلى قيم سالبة. في هذه الدراسة تم قياس مقاومة الاحتكاك الداخلية والخارجية. وجد أن حالة التربة وكثافة التسارع كلاهما لهما تأثير ملحوظ على عملية الفشل. كذلك تم تضمين تقدير تقريبي للازا حات طويلة الأجل على سطح التربة المهتز في نتائج هذا البحث.

الكلمات المفتاحية: الحمل الزلزالي, عناصر محدودة ثلاثي الأبعاد, مقاومة الاحتكاك, الازاحة الطولية.

1. INTRODUCTION

The earthquake, one of the worst natural disasters ever, caused significant damage and loss of life. Likewise, at this moment, earthquakes are unpredictable and unmanageable. The only possible choice available to engineers is to design and construct structures in a manner that eliminates the impact of earthquakes (**Arora, 2004; Al-Busoda and Al-Rubaye, 2015; Fattah et al., 2016; Albusoda and Alsaddi, 2017; Mahmoud and Al-Baghdadi, 2018; Al-Salakh and Albusoda, 2020; Salih et al., 2020; Zheng et al., 2022; Yang et al., 2022**) or to make an effort to mitigate seismic effects through soil treatment and mitigation. The axial force resulting from inertial and kinematic impacts, the inertial load attributed to the superstructure, and other loads associated with kinematic consequences (ground movement) are the major driving loads to a pile throughout such seismic situations. The 1-g shaking table test is widely employed to examine the ground's dynamic motion and earthquake-damaged soil structures' responses. A shaking table is used to replicate the earthquake-related shaking.

The ultimate strength of long piles in frictional soil, frequently utilized in offshore projects, is strongly influenced by pile FR. According to (**Vesic, 1970),** the shaft resistance a long pile creates varies with pile depth. It usually increases with pile penetration depth till achieving a peak value a short distance above the pile tip, after which exterior skin resistance starts to

drop dramatically at the zone above the pile tip, as seen in **Fig. 1a**. This was attributed to the 'Arching effect,' which restricted effective lateral stresses. The pattern of shaft resistance in sandy soil for various pile lengths is depicted in this diagram. (**Vesic, 1970; Fellenius and Altaee, 1995; Klotz and Coop, 2001)** proposed that the maximum possible FR was measured at a point above the pile tip.

To evaluate the response of piles under lateral stresses, various research used laboratory tests **(Fattah et al., 2017; Fattah et al., 2021; Al-Salakh and Albusoda, 2020; Hussein and Albusoda, 2023; Hussein and El Naggar, 2023; Alzabeebee and Keawsawasvong, 2023)** and the three-dimensional (3D) finite element approach **(Al-Jeznawi et al., 2022a and 2022b)**. FR for piles built in homogeneous sand does not rise linearly with pile depth and is dependent on lateral stresses. Based on this pattern, the highest FR may be anticipated above the pile base. Owing to such an increase in shear displacement, (**DeJong et al., 2003)** reported that the radial distance of the shear zone surrounding the outer face of the pile is produced with a thickness ranging from (3.5 mm to 5.5 mm) for silica sand. The thin shear zone interfaces interpret the load formation and transmissions along the external shaft of the pile through the shear zone. Increased lateral pressure could be caused by an increase in limitation imposed by the surrounding soil, which could modify the volume of the thin shear zone. Thus, (**Al-Soudani, 2020)** stated that the pile FR distribution differs from the researchers' point of view and from one test to another, which led to high discrepancies in design approaches of friction distribution. **Table 1** summarizes the allowable movement limits required for resistance mobilization according to the standardizations.

Table 1. The required Allowable movement limits for pile resistance mobilization.

Author (s)	Soil	Pile friction capacity	Point tip capacity
(Vesic, 1970)	**sand**	**0.08*D**	
(Kulhawy, 1984)	**sand**	**(10 to 20) mm**	
(German Institute for Standardization, 1990)	**all**	**(10 to 20) mm**	**More than 10 mm**
(Fleming et al., 2008)	**all**	**0.005*D to 0.02*D**	**0.05*D to 0.1*D**
(Briddle and Yandzio, 2003)	**all**	**(7 to 10) mm**	**More than 40 mm**
(Canadian Geotechnical Society, 2006)	**all**	**(5 to 10) mm**	**0.05*D to 0.1*D**
(John et al., 2012)	**all**	**Pile FR needs less displacement to mobilize than pile tip capacity**	
(Wu et al., 2020)	**all**	**(25 to 10) mm**	**0.1*D for driven pile 0.3*D for bored pile**

Iraqi experts have been researching pile foundations in the sand under various shaking patterns of motion due to increased seismic activity in the last few years. Likewise, pipe piles are frequently used as they are simpler and more affordable to build, can be tested for safety before being established, and may be tailored to meet certain load specifications, thus saving money by reducing the need for extra reinforcing.

Hence, in this study, using MIDAS GTS NX finite element software, the effects of static vertical and lateral stresses with three distinct seismic vibrations on the soil-pipe pile configuration about the kinematic interaction were investigated. The program findings were validated using (**Hussein and Albusoda, 2021)** laboratory findings.

2. NUMERICAL MODELING

Three-dimensional finite element models have been developed using the MIDAS GTS NX software, considering the shaking load nonlinearity. (**Al-Jeznawi et al., 2022a)** explained the laboratory experiments, meshing, static and dynamic boundary conditions, and validation of the constitutive models used in their latest work. The present computer analysis included a full-scale model and three recorded earthquake data (Kobe, Halabja, and Ali Algharbi). (**Hussein and Albusoda, 2021)** performed a 1g shaking table experiment to assess a closed-ended Aluminum pipe pile constructed in two different soil layers. The present numerical models were compared with the laboratory observations **(Al-Jeznawi et al., 2022a; Al-Jeznawi et al., 2022c)** and reported the validation outcomes.

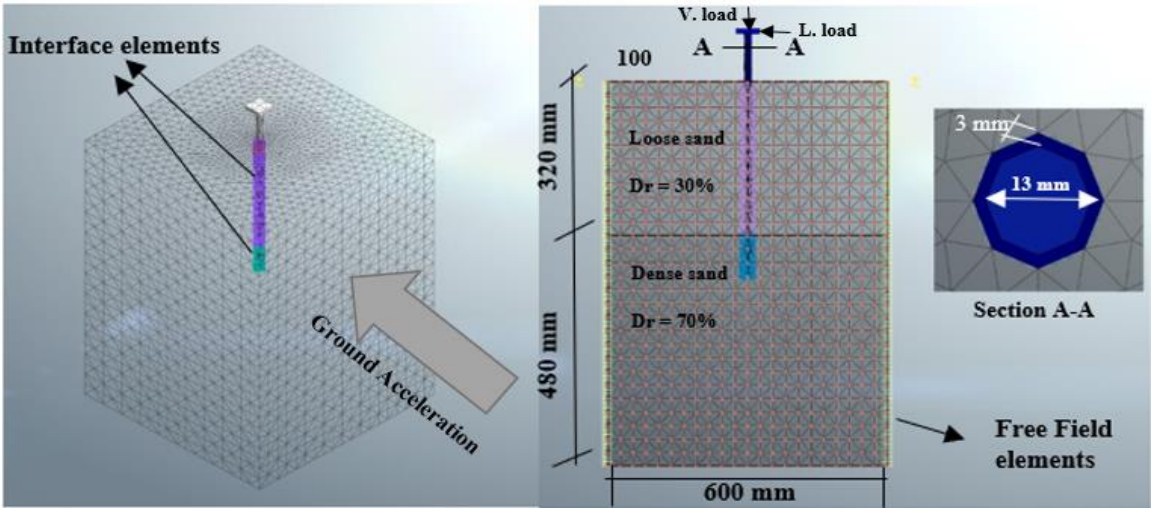

Figure 1. The implemented finite element model in the current study (**Al-Jeznawi et al., 2022a)**.

3. MODEL DESCRIPTION

The current study adopted an open-ended aluminum pipe pile with three earthquake records (PGA = 0.82, 0.102, and 0.1 g) and pile L/D =25. The pipe piles are set in cohesionless two soil layers (D_r = 30% and 70% as the upper and bottom layers, respectively). The soil characteristics have been adopted from (**Hussein and Albusoda, 2021),** who performed physical laboratory tests using air-dried poorly graded sand (SP). These characteristics have been calibrated using (**Beaty and Byrne, 2011)** approach. The equivalent SPT blow count for clean sand $(N_1)_{60}$, obtained as per ASTM D 1586-99, is the fundamentals of the basic calibration formulas **(Beaty and Byrne, 2011)**. The model has been exposed to the total allowable vertical load and 50% of the allowable lateral load, as shown in **Fig. 1**. These static loads were applied as point loads on the pile cap. The main input parameters for the soil and pile materials are presented in **Tables 2 and 3.**

The pile element's constitutive relationship was linear elastic. An extensive study uses an interconnection component with restricted shear resistance to demonstrate the relationship between the pile and the surrounding soil, employing the Modified Mohr-Coulomb failure criteria. The normal and shear coefficients of the interface elements were estimated. Regarding the two-layer soil medium with an upper layer of sand that is 11.2 m thick and a

bottom layer that is 28 m thick, a 0.56 m diameter pile is constructed. The core pile is assumed to have descended into the deep sand below after reaching the subsoil.

Table 2. Soil characteristics (**Hussein and Albusoda, 2021)**.

Properties	D_r = 30%	D_r = 70%
G (kPa)	5000	380,000
ν	0.25	0.3
Ø (°)	32	35
D_r (%)	30	70
Gs (unitless)	2.64	2.64
k (cm/sec)	5.6×10^{-3}	5.6×10^{-3}
ψ (°)	2	5

Table 3. Pile characteristics **(Hussein and Albusoda, 2021)**.

Properties	Pile shaft
Material	Aluminium
Size (m)	D_o = 0.56, D_i = 0.455, L = 17.5
Slenderness ratio	25
γ (kN/m^3)	30
E (GPa)	67
I (m^4)	4.36×10^{-8}
A (m^2)	2.7×10^{-4}
ξ (%)	5

4. PILE AXIAL RESPONSE

Numerous infrastructure and construction failures following earthquakes have been connected with notable settlements **(Tokimatsu et al., 1998)**. Due to the increased pore pressure the loose sand creates, the soil shear stiffness and effective vertical stress are reduced when piles are installed in saturated sand layers. Additionally, there will be different effects on the end bearing and pile shaft's friction resistance. The higher-end bearing capacity could be activated due to the pile settling dramatically when additional pore pressure in the bearing stratum increases. Conversely, shaft friction reduces with the creation of excess pore pressure and may potentially vanish once liquefaction occurs. Yet, the nature of damage differs in dry-site piles. The pile may experience intense compression and tension stages, and the settlement may occur during rapid acceleration. However, pile settling is less than in saturated places, and bearing capacity failure is improbable because compaction may increase the soil's characteristics. Following is a discussion of how the acceleration intensity affects FR and open-ended pipe pile settlement for both saturated and dry models .

Fig. 2 displays the time history of the OE Aluminum pipe pile's vertical movement in both wet and dry models. Unlike the preceding models, the saturated models showed noticeably higher settlements than the dry models, independent of the acceleration histories.

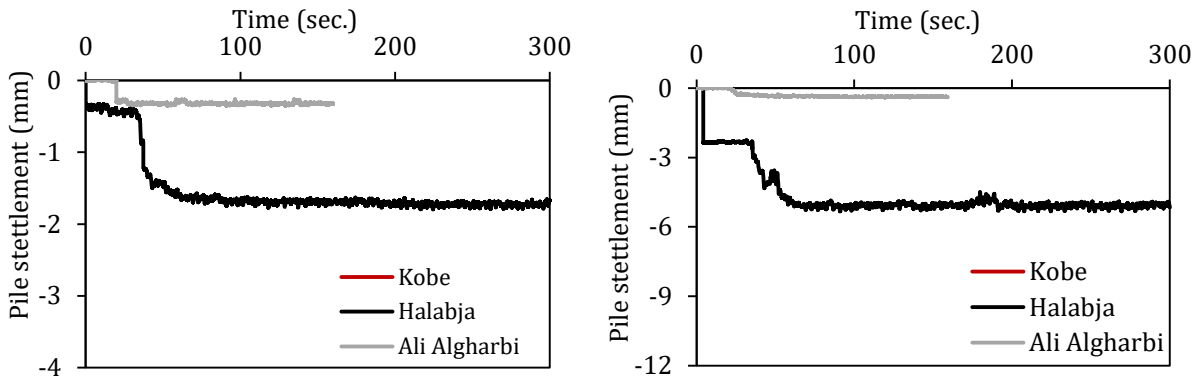

(a) Dry case (b) Saturated case

Figure 2. Pile settlement embedded in layered soil during the shaking of different acceleration histories.

Table 4 summarizes the modeling findings for the soil plug resistance and the highest value of adjacent soil resistance when static stress alone and mixed static-seismic load were applied, respectively. (i.e., the Kobe earthquake).

Table 4. The numerical results of the plug and the surrounding soil resistance under static and Kobe earthquakes (PGA = 0.82g).

State	Dry		Saturated	
	Max. resistance of the plug soil (MPa)	Max. resistance of the soil below the pile tip (MPa)	Max. resistance of the plug soil (MPa)	Max. resistance of the soil below the pile tip (MPa)
After applying the vertical static load only	-15.34	14.1	-8.4	7.9
During applying the combined static-dynamic load - at the PGA	-16.56	15.4	-10.2	9.6
After applying the combined static-dynamic load- at the final stage	-14.6	13	-8	6.9

While seismic activation reduced the arching within the soil plug, a higher resistance than the maximum resistance of the soil next to it was found. It is crucial to emphasize that the soil plug's length was preserved at 4D since the author observed that when employing a plug length of 3D, the length is insufficient for plugging mode because the sand keeps sliding up within the pipe pile, as illustrated in **Fig. 3a**. As a result, the pile collapsed in the plugged mode (as a CE pipe pile) by using $4*D_{inner}$, and no more soil was seen to go into the pipe pile, as demonstrated in **Fig. 3b**. This could have been explained by the existence of a loose soil layer (D_r of 30%); hence an additional soil plug was necessary to attain high soil particle density within the pipe pile.

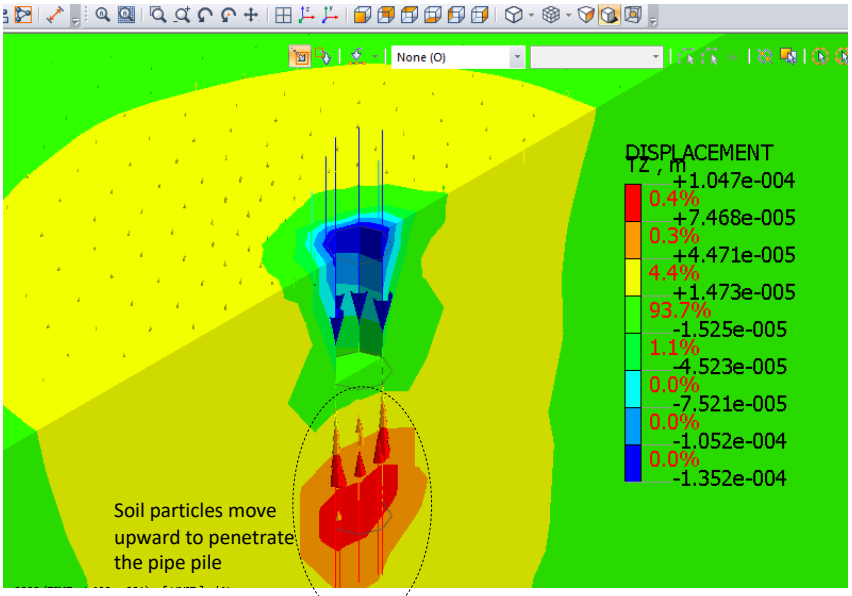

(a)Length of the plug soil 3*D_{inner}

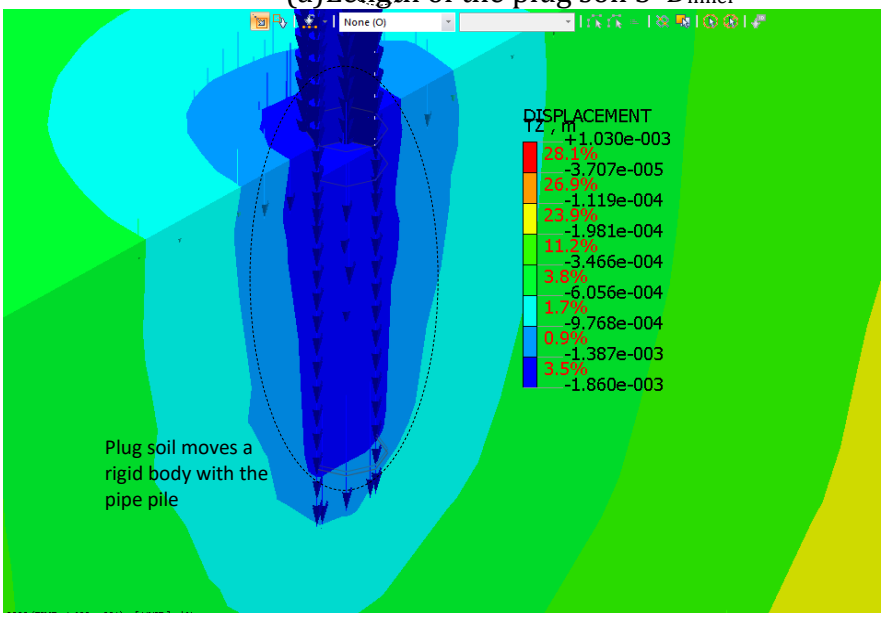

(b) Length of the plug soil 4*D_{inner}

Figure 3. Plugging soil moving direction at the end of applying the static-seismic loading.

Their findings demonstrated that the plug resistance is fully mobilized at the zone 20% of the plug length from the pile tip, just like the other models performed by (**Al-Jeznawi et al., 2022a)**. The largest plug resistance in all models is between 0 and around 20% of the total plug length, as shown in **Fig. 4**.

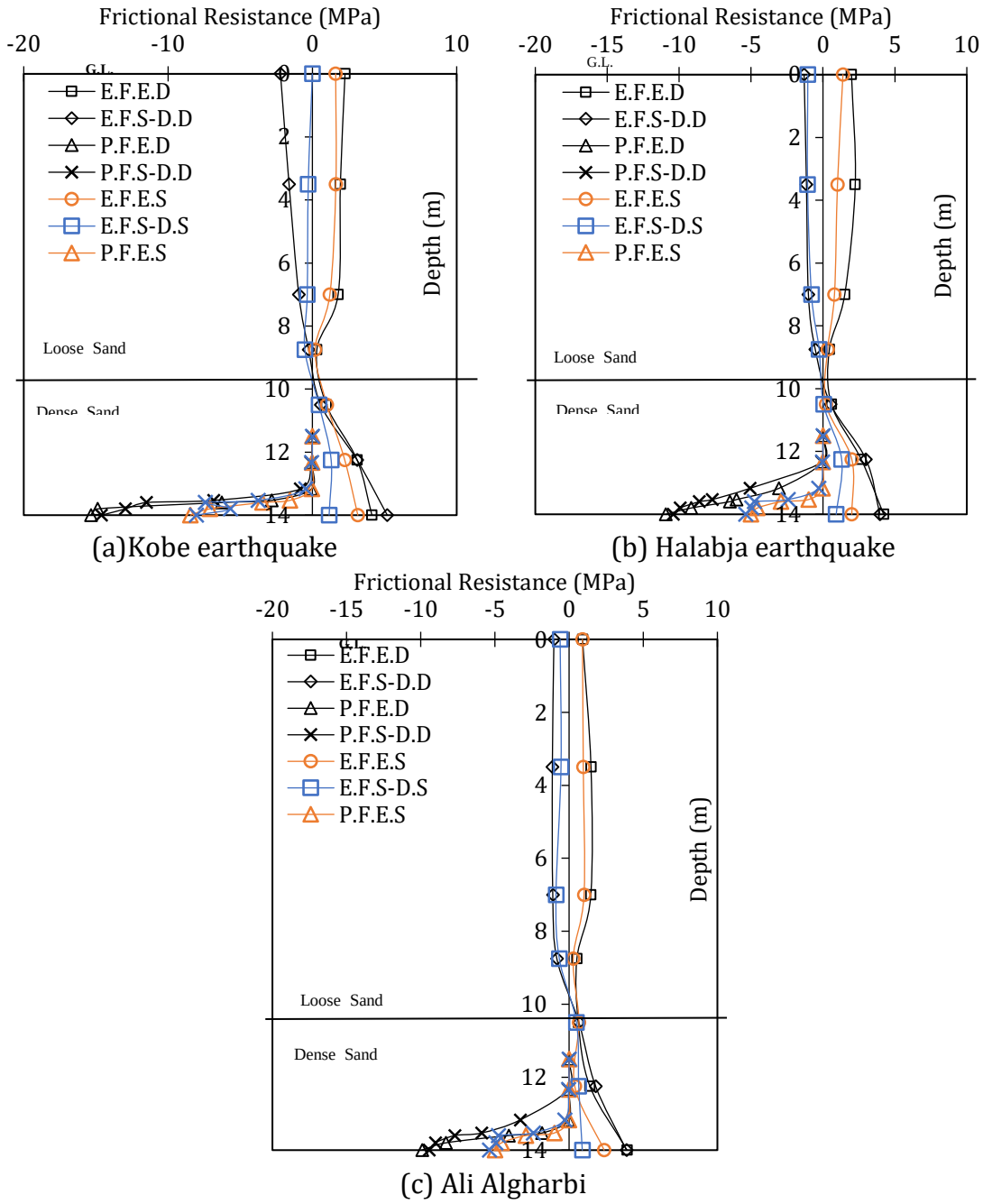

Figure 4. Internal and external FRs of the OE Aluminum pipe pile embedded in layered soil (PGA of 0.82 g).

5. CONCLUSIONS

This research investigates the acceleration intensity effects on the seismic response of an open-ended pipe pile set in dry and saturated sand soils. The main variables were adjusted depending on the modified Mohr-Coulomb model. The primary findings of the current study were verified with 1 g shaking table tests. The results of the present study indicate that the soil's shear strength is reduced with the release of excess pore pressure. The pile is anticipated to drop due to the development of high pore-water pressure (liquefaction

commencement). At this point of the 1g laboratory tests, it was observed that soil particles had generally lost their shear strength and behaved roughly like a slurry. The pile frictional resistance decreased significantly (i.e., about 45% under the effect of the Kobe earthquake) when the ground condition shifted from dry to fully saturated. The computer simulations simulated this effect by considerably lowering the FR during the dynamic excitation until it reached the lowest possible value at the end. A significant mass circulates near the pile tip due to the soil plug arching and densification. The pile underwent noticeable deformations caused by a large drop in soil stiffness as the nearby loose sand soil exhibited liquefaction (excess pore water pressure ratio > 85%). Overall, the frictional resistance surrounding the pile body was less than that at the pile base, i.e., under the effect of the Kobe earthquake, the decreasing ratios were about 11% and 14% for the dry and saturated soil conditions, respectively.

NOMENCLATURE

Symbole	Description	Symbole	Description
A	Pile cross-section area	γ	Unite weight
3D	Three-dimensional.	*I*	Moment of inertia
D_{50}	Diameter of the average grain size	ξ	Damping ratio
D_i	Inner pile diameter	ψ	Dilatancy angle
D_o	Outer pile diameter	OE	Open-ended
D_r	Relative displacement	E.F.S-D.D	External frictional resistance under the static-dynamic load of pipe pile embedded in dry soil
FR	Frictional resistance	P.F.S-D.D	Plug (internal) frictional resistance under the static-dynamic load of pipe pile embedded in dry soil.
G_s	Specific gravity	E.F.S-D.S	External frictional resistance under the static-dynamic load of pipe pile embedded in saturated soil
k	Permeability	P.F.S-D.S	Plug (internal) frictional resistance under the static-dynamic load of pipe pile embedded in saturated soil.
L/D	Slenderness ratio		
$(N_1)_{60}$	Equivalent SPT blow count for clean sand	PGA	Peak ground acceleration.

REFERENCES

Al-Busoda, B.S., and Al-Rubaye, A.H., 2015. Bearing capacity of bored pile model constructed in gypseous soil. *Journal of Engineering*, 21(3), pp. 109–128. Doi:10.31026/j.eng.2015.03.07.

Albusoda, B.S., and Alsaddi, A.F., 2017. Experimental study on performance of laterally loaded plumb and battered piles in layered sand. *Journal of Engineering*, 23 (9), pp. 23-37. Doi:10.31026/j.eng.2017.09.02

Al-Jeznawi, D., Mohamed J. I. B., Albusoda, B. S., and Khalid, N., 2022a. Numerical modeling of single closed and open-ended pipe pile embedded in dry soil layers under coupled static and dynamic

loadings. *Journal of the Mechanical Behavior of Materials*, 31(1), pp. 587-594. Doi:10.1515/jmbm-2022-0055

Al-Jeznawi, D., Jais, I.B.M., Albusoda, B.S., Alzabeebee, S., Keawsawasvong, S., Khalid, N., 2022b. Numerical study of the seismic response of closed-ended pipe pile in cohesionless soils. *Transportation Infrastructure Geotechnology*. pp. 1-27. Doi:10.1007/s40515-022-00273-z

Al-Jeznawi, D., Jais, I.B.M., and Albusoda, B.S., 2022c. A soil-pile response under coupled static-dynamic loadings in terms of kinematic interaction. *Civil and Environmental Engineering*, 18 (1), pp. 96-103. Doi:10.2478/cee-2022-0010

Al-Salakh, A.M., and Albusoda, B.S., 2020. Experimental and theoretical determination of settlement of shallow footing on liquefiable soil. *Journal of Engineering* 26 (9), pp. 155-164. Doi:10.31026/j.eng.2020.09.10

Al-Soudani, W.H., 2020. Evaluating the performace of new techniques for open-ended pipe piles in dry sandy soil. Baghdad. Ph.D. Thesis, University of Baghdad.

Altaee, A., and Fellenius, B.H., 1994. Physical modeling in sand. *Canadian Geotechnical Journal*, *31*(3), pp. 420-431. Doi:10.1139/t94-049

Alzabeebee, S., and Keawsawasvong, S., 2023. Sensitivity of the seismic response of bored pile embedded in cohesionless soil to the soil constitutive model. *Innovative Infrastructure Solutions*, *8*(1), p.7. Doi:10.1007/s41062-022-00988-5

Arora, K. R., 2004. Soil mechanics and foundation engineering. Standard Publishers Distributors, Delhi, pp. 69-257.

Beaty, M., and Byrne, M.P., 2011. Documentation Report: UBCSAND constitutive model on itasca udm web site.

Briddle, T., and Yandzio, E., 2003. Steel Designers Manual-6th edition. Blackwell Publishing: Steel Construction Institute SCI.

Canadian Geotechnical Society, 2006. Canadian Foundation Engineering Manual, 4th ed.; Canadian Geotechnical Society, Vancouver, B.C.

DeJong, J., Randolph, M., and White, D., 2003. Interface load transfer degradation during cyclic loading: a microscale investigation. *Soils and foundations*, *43*(4), pp. 81–93. Doi:10.3208/sandf.43.481

Fattah, M.Y., Zabar, B.S., and Mustafa, F.S., 2017. Vertical vibration capacity of a single pile in dry sand. *Marine Georesources and Geotechnology,* 35(8), pp. 1111-1120. Doi:10.1080/1064119X.2017.1294219

Fattah, M.Y., Zbar, B.S., and Al-Kalali, H.H.M., 2016. Three-dimensional finite element simulation of the buried pipe problem in geogrid reinforced soil. *Journal of Engineering*, 22(5), pp. 60–73. Doi:10.31026/j.eng.2016.05.05.

Fattah, M.Y., Zbar, B.S., Mustafa, F.S., 2021. Effect of soil saturation on load transfer in a pile excited by pure vertical vibration. *Proceedings of the Institution of Civil Engineers–Structures and Buildings*, 17(2), pp. 132–144. Doi:10.1680/jstbu.16.00206.

Fleming, K., Weltman, A., Randolph, M., and Elson, K., 2008. *Piling engineering*. CRC press.

German Institute for Standardization, 1990. Bored cast-in-place piles; formation, design and bearing capacity. https://books.google.iq/books?id=1H7ToAEACAAJ

Hussein, A.F., and El Naggar, M.H., 2023. Dynamic performance of driven and helical piles in cohesive soil. *Acta Geotechnica*, *18*(3), pp. 1543-1568. Doi:10.1007/s11440-022-01649-8

Hussein, R.S., and Albusoda, B.S., 2022. Behavior of group piles under combined loadings after improvement of liquefiable soil with nanomaterials. *Journal of the Mechanical Behavior of Materials,* 31(1), pp. 639-648. Doi:10.1515/jmbm-2022-0059

Hussein, R., and Albusoda, B., 2021. Experimental and numerical analysis of laterally loaded pile subjected to earthquake loading. *Modern Applications of Geotechnical Engineering and Construction*, pp. 291-303. Doi:10.1007/978-981-15-9399-4_25

Idriss, I.M., and Boulanger, R.W., 2010. SPT-Based liquefaction triggering procedures. Department of Civil and Environmental Engineering, University of California Davis, California.

John, B., Tim, C., Hilary, S., and Michael, B., 2012. ICE manual of geotechnical engineering: Volume II. https://www.icevirtuallibrary.com/doi/abs/10.1680/moge.57098

Klotz, E.U., and Coop, M.R., 2001. An investigation of the effect of soil state on the capacity of driven piles in sands. *Géotechnique*, *51*(9), pp. 733-751. Doi:10.1680/geot.2001.51.9.733

Kulhawy, F., 1984. Limiting tip and side resistance: fact or fallacy. In Analysis and Design of Pile Foundations. San Francisco, Calif: American Society of Civil Engineers, pp. 80-98

Mahmoud, T.K., and Al-Baghdadi, H.A., 2018. Seismic response of nonseismically designed reinforced concrete low rise buildings. *Journal of Engineering*, 24(4), pp. 112–127. Doi:10.31026/j.eng.2018.04.08.

Paikowsky, S.G., and Whitman, R.V., 1990. The effects of plugging on pile performance and design. *Canadian Geotechnical Journal*, *27*(4), pp. 429-440. Doi:10.1139/t90-059

Salih, S.J.H., Salih, N.B., Noory, D.B., and kawa Abdalqadir, Z., 2020. Load-settlement behavior of steel piles in different sandy soil configurations. *Journal of Engineering*, *26*(10), pp. 109-122. Doi:10.31026/j.eng.2020.10.08.

Tokimatsu, K., 1998. Effects of lateral ground movements on failure patterns of piles in the 1995 Hyogoken-Nambu earthquake. In *Proc. A Speciality Conf., Geotechnical Earthquake Engineering and Soil Dynamics III*. pp. 1175–1186

Vesic, A.S., 1970. Tests on instrumented piles, Ogeechee River site. *Journal of the Soil Mechanics and Foundations Division*, 96(2), pp. 561-584. Doi:10.1061/JSFEAQ.0001404

Wu, J., Kouretzis, G., Suwal, L., Ansari, Y., and Sloan, S.W., 2020. Shallow and deep failure mechanisms during uplift and lateral dragging of buried pipes in sand. *Canadian Geotechnical Journal*, *57*(10), pp. 1472-1483. Doi:10.1139/cgj-2019-028

Yang, X., Zhang, Y., Liu, H., Fan, X., Jiang, G., El Naggar, M.H., Wu, W., and Liu, X., 2022. Analytical solution for lateral dynamic response of pile foundation embedded in unsaturated soil. *Ocean Engineering*, 265, P.112518.

Zheng, C., Luo, T., Kouretzis, G., Ding, X., and Luan, L., 2022. Transverse seismic response of end-bearing pipe piles to S-waves. *International Journal for Numerical and Analytical Methods in Geomechanics. 46*(10), pp. 1919-1940. Doi:10.1002/nag.3374